



# Roman Coronagraph Instrument Reference Information

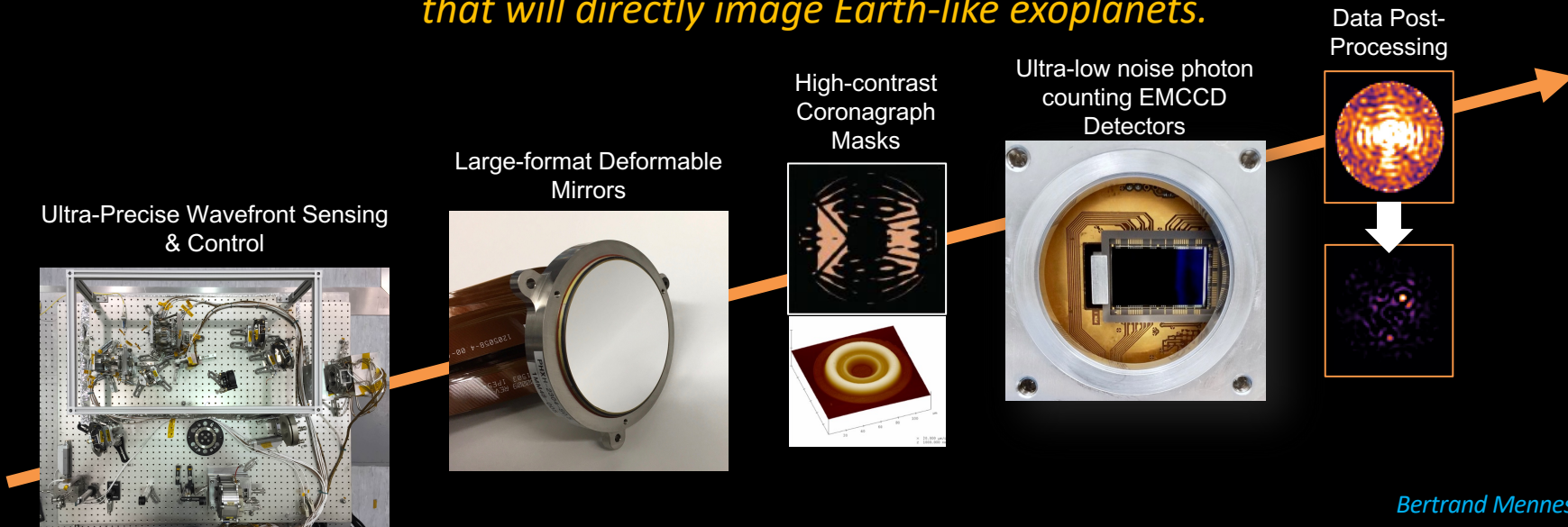
February 2021

*Information here captures the instrument design elements  
as of the CGI Preliminary Design Review in September 2019.*

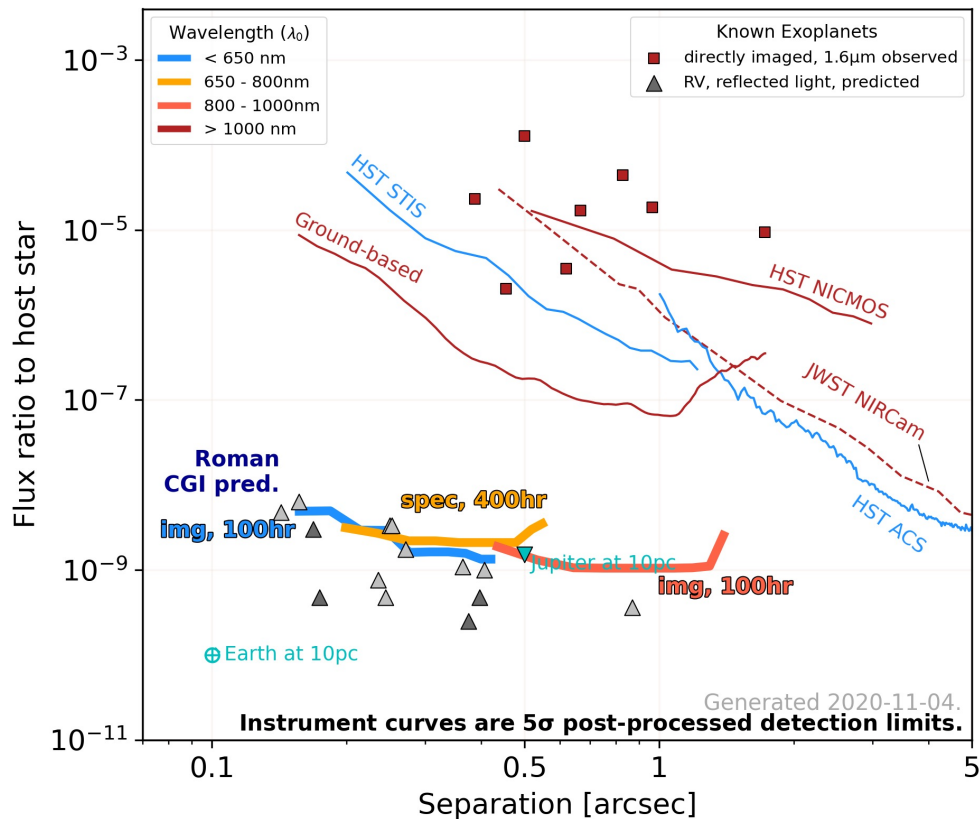
Roman/CGI Science and Engineering Project Teams  
Jet Propulsion Laboratory, California Institute of Technology

# Critical Technology Demonstrations

*CGI is an advanced technology demonstrator for future missions that will directly image Earth-like exoplanets.*

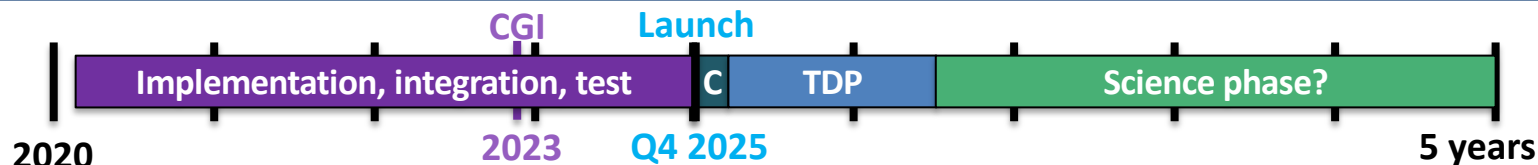


**CGI will premiere in space the technologies needed by future missions to image and characterize rocky planets in the habitable zones of nearby stars. By demonstrating these tools in a system with end-to-end, scientific observing operations, NASA will reduce the cost and risk of a potential future flagship mission.**



Instrument performance requirements and current-best-estimated performance are based on laboratory demonstrations and model predictions, as of November 11, 2020. Laboratory demonstrations and model refinements are ongoing.

See V. Bailey,  
<https://github.com/nasavbailey/DI-flux-ratio-plot> for a detailed description of this plot.



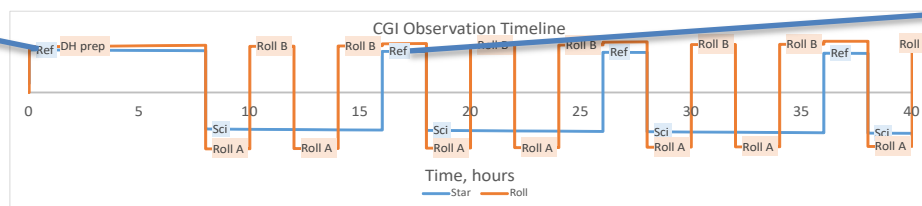
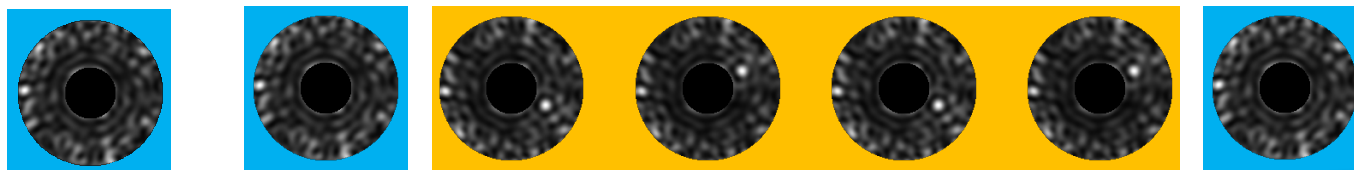
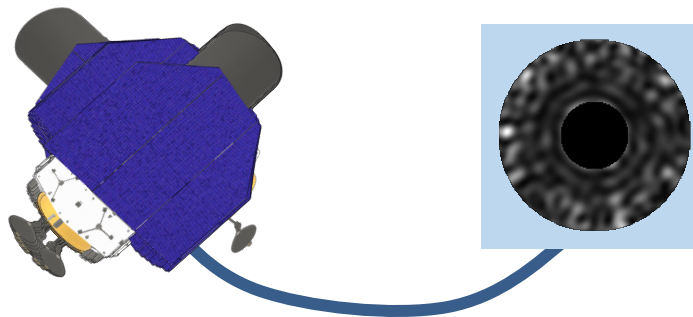
- **Feb 2020: Entered implementation phase (Phase C)**
- **Q3 2023: Instrument delivery to payload integration & test**
- **Q4 2025: Launch**
- **Commissioning Phase**
  - 450 hr in first 90 days after launch
- **Technology Demonstration Phase (TDP)**
  - **~2200 hr (3 months) baselined** in next 1.5 years of mission
- **If TDP successful, potential science phase**
  - 10-25% of remainder of 5 year mission
  - Commission unofficial observing modes (add'l mask+filter combo's)
  - Support community engagement
  - **Not guaranteed: would require additional resources**
  - Starshade rendezvous, if selected



# Potential Technology Demonstration Phase Observations

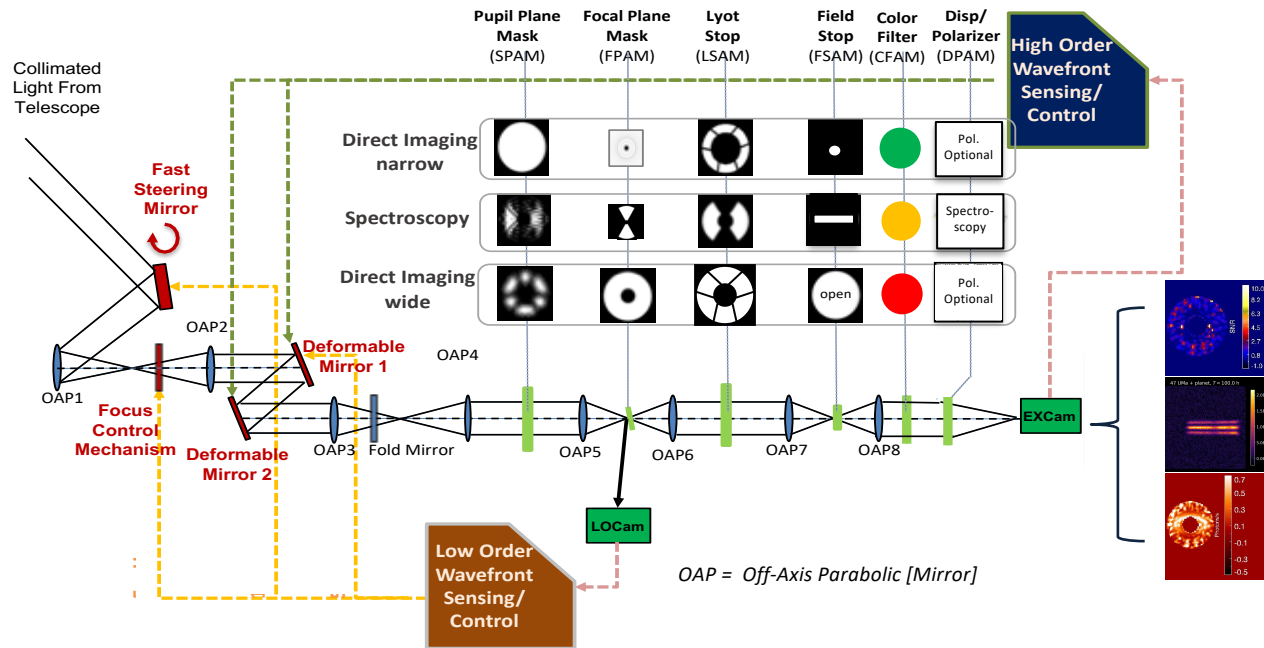
- Self luminous planet image and spectra
- Reflected light planet image and spectrum
- Bright debris disk polarimetry
- Faint debris disk detection

# CGI Observing Scenario

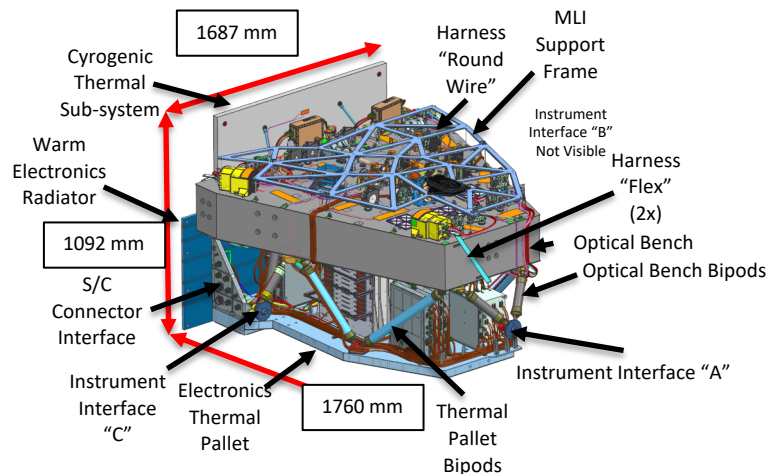


John Krist (JPL)

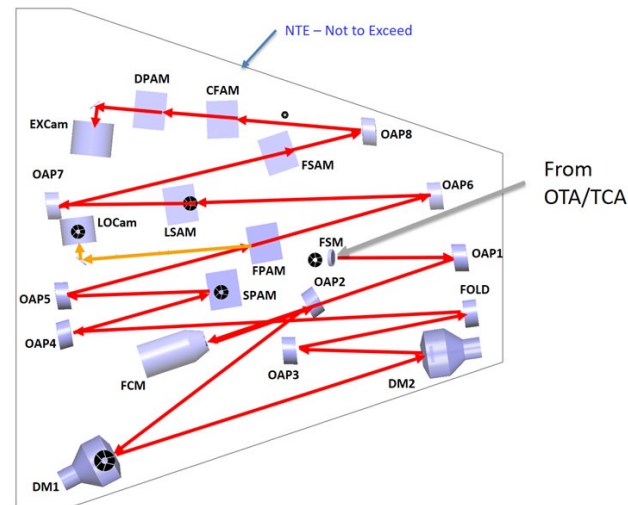
# CGI Architecture



- Three observation modes implemented with three different sets of masks/filters
- Share the same optical beam train, with two wavefront control loops to achieve high contrast (better than 1E-8)



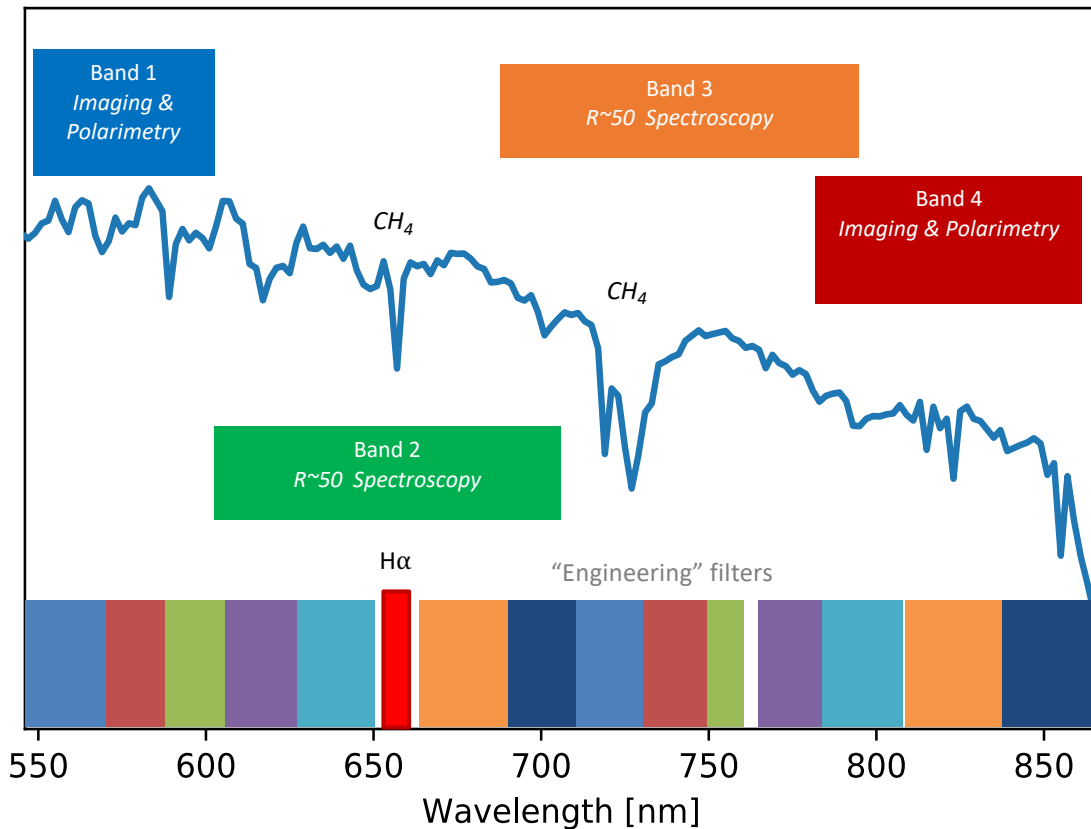
- In the WFIRST Payload, CGI mounts onto the Instrument Carrier (IC) shared with the Wide Field Instrument. The Tertiary Collimator Assembly (TCA; not shown) is the optical interface between the telescope and CGI, and relays an exit pupil onto the Fast Steering Mirror (FSM).
- Phase C design as of November 2020.



- The first deformable mirror, **DM 1**, is positioned at a relay pupil following the **FSM**. **DM 2** is positioned 1 meter away to enable correction of amplitude errors and phase errors originating from out-of-pupil surfaces.
- Both coronagraph mask types, the Hybrid Lyot and Shaped Pupil Coronagraphs (HLC and SPC), are implemented on the same optical beam train and selected by changing masks at the planes labeled **SPAM**, **FPAM**, **LSAM**, and **FSAM**.
- Observing mode is selected by mechanisms after the Lyot stop.



# CGI Passbands



Three “official” modes will be fully tested prior to launch (Bands 1, 3, and 4)

Additional modes installed but not fully tested before launch

# CGI Observing Modes

Three “official” modes will be fully tested prior to launch.

$\lambda_{\text{center}}$ (nm)	FWTB	Mode	FOV radius	Polarimetry?
575	10.1%	Imager	0.14” – 0.45”	Y
730	15.1%	Slit + R~50 Prism	0.18” – 0.55”	-
825	9.9%	Imager	0.45” – 1.4”	Y

# CGI Narrowband Modes

Additional modes installed but not fully tested before launch

$\lambda_{\text{center}}$ (nm)	FWTB	Mode	FOV radius	Polarimetry?
660	15.2%	Slit + R~50 Prism	0.17" – 0.5"	Y
H $\alpha$	0.4%	Imager	0.17" – 0.5"	Y



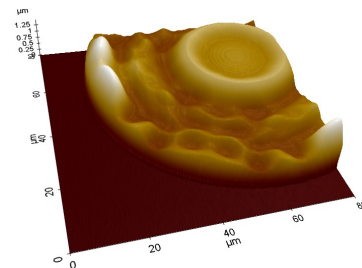
# CGI Narrowband Modes

Wavefront Control Engineering Bandpasses (2.5-3.5%) installed

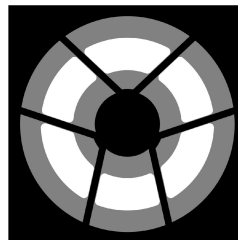
Name	$\lambda_{\min}$ [nm]	$\lambda_0$ [nm]	$\lambda_{\max}$ [nm]	FWTB [%]	width [nm]
<b>1a</b>	540	550	560	2.5	20
<b>1b</b>	564.5	575	585.5	2.6	21
<b>1c</b>	588	599	610	2.7	22
<b>2a</b>	604	615	626	2.6	22
<b>2b</b>	629	638	647	1.9	18
<b>2c</b>	653	656.3	659.6	0.4	6.6
<b>3a</b>	669	681	693	2.6	24
<b>3b</b>	692	704	716	2.6	24
<b>3c</b>	717	727	737	2.0	20
<b>3g</b>	739.5	752	764.5	2.5	25
<b>3d</b>	750.25	754	757.75	0.5	7.5
<b>3e</b>	764	777.5	791	2.7	27
<b>4a</b>	778	792	806	2.8	28
<b>4b</b>	810	825	840	2.9	30
<b>4c</b>	842	857	872	2.8	30

# Hybrid Lyot Coronagraph

- The HLC provides a full 360° high contrast field of view.
- Focal plane occulting mask is a circular,  $r = 2.8 \lambda_c/D$  partially-transmissive nickel disc overlaid with a PMGI dielectric layer with a radially and azimuthally varying thickness profile.
- The HLC design incorporates a numerically optimized, static actuator pattern applied to both deformable mirrors.
- Lyot stop is an annular mask that blocks the telescope pupil edges and struts.

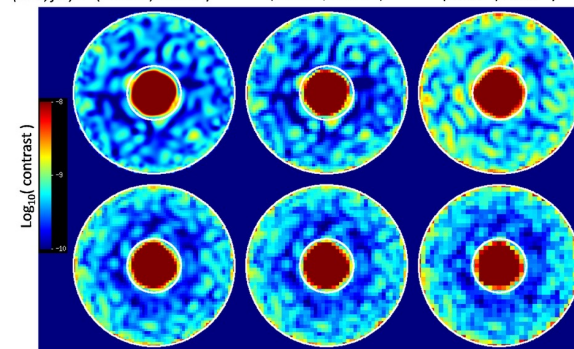


**HLC occulting mask.** AFM surface height measurement of an occulting mask fabricated by the JPL Micro Devices Lab. Recent design refinements include azimuthal ripples in thickness of the dielectric, which extends across the field of view.



**HLC Lyot stop.** Diagram of Lyot stop model: white represents the transmitted region; black represents the telescope pupil; gray represents the region blocked by the stop in addition to the telescope pupil.

9 wavelengths, perfect knowledge $0.2 \lambda_c/D$ point sampling (Inner, full) = $(3.8 \times 10^{-10}, 4.2 \times 10^{-10})$	9 x 1.1% sub-bands, probing, $0.3 \lambda_c/D$ finite pixels ( $4.2 \times 10^{-10}, 4.6 \times 10^{-10}$ )	2 x 5% sub-bands, probing, $0.3 \lambda_c/D$ finite pixels ( $9.0 \times 10^{-10}, 7.8 \times 10^{-10}$ )
---	--	--



3 x 3.3% sub-bands, probing, $0.3 \lambda_c/D$ finite pixels ( $3.3 \times 10^{-10}, 5.0 \times 10^{-10}$ )	3 x 3.3% sub-bands, probing, $0.4 \lambda_c/D$ finite pixels ( $3.2 \times 10^{-10}, 5.3 \times 10^{-10}$ )	3 x 3.3% sub-bands, probing, $0.5 \lambda_c/D$ finite pixels ( $3.3 \times 10^{-10}, 5.5 \times 10^{-10}$ )
--	--	--

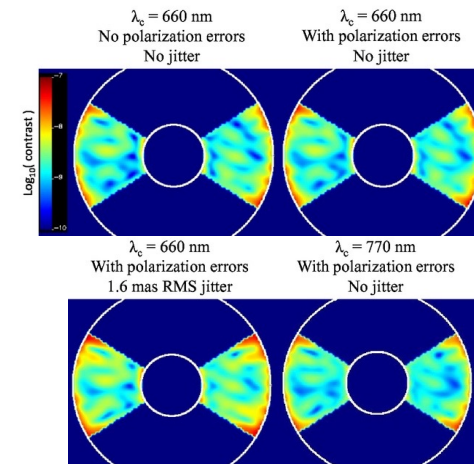
Simulated HLC PSF including aberrations and high-order wavefront control operations, illustrating the annular dark zone between 3 and  $9 \lambda_c/D$ . Each sub-panel represents a different scenario for DM probe wavelength resolution and detector sampling.

## References

- J. Trauger, D. Moody, et al., JATIS Vol 2, id. 011013 (2016) - <https://doi.org/10.1117/1.JATIS.2.1.011013>
- J. Krist, et al., Proc SPIE Vol 10400, id. 1040004. (2017) - <http://dx.doi.org/10.1117/12.2274792>
- K. Balasubramanian, et al., Proc SPIE Vol 10400, id. (2017) - <https://doi.org/10.1117/12.2274059>

# Shaped Pupil Coronagraph

- The shaped pupil apodizer is a reflective mask on a silicon substrate with aluminum regions for reflection and black silicon regions for absorption.
- The hard-edged occulting mask has either a bowtie-shaped opening for characterization (spectroscopy) mode or an annular aperture for debris disk imaging.
- The SPC Spectroscopy designed in 2017 produces a  $2 \times 65^\circ$  bowtie dark zone from  $3.0 - 9.1 \lambda_c/D$  over a 15% bandpass.
- The SPC Wide Field of View design produces a  $360^\circ$  dark zone from  $5.9 - 20.1 \lambda_c/D$  in a 10% bandpass.



Spectroscopy SPC (2017 design) simulations at  $\lambda_c = 660$  and  $770$  nm including system aberrations, pointing jitter, and wavefront control operations. The circles correspond to  $r = 3$  and  $9 \lambda_c/D$ .

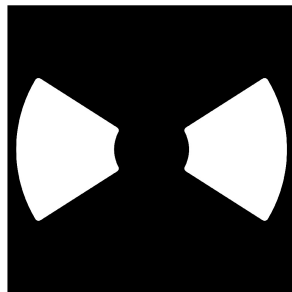
## References

- N. T. Zimmerman, et al., JATIS Vol 2 id. 011012 (2016) - <http://dx.doi.org/10.1117/1.JATIS.2.1.011012>
- K. Balasubramanian, et al., JATIS Vol2 id. 011005 (2015) - <https://doi.org/10.1117/1.JATIS.2.1.011005>
- A. J. E. Riggs et al., N. T. Zimmerman, et al., Proc SPIE Vol 10400 (2017) - <http://dx.doi.org/10.1117/12.2274437>
- J. Krist, et al., Proc SPIE Vol 10400, id. 1040004. (2017) - <http://dx.doi.org/10.1117/12.2274792>

Apodizer Mask



Focal Plane Mask

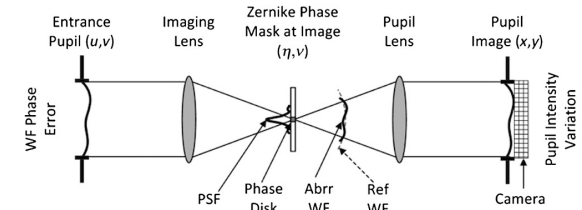


Lyot Stop

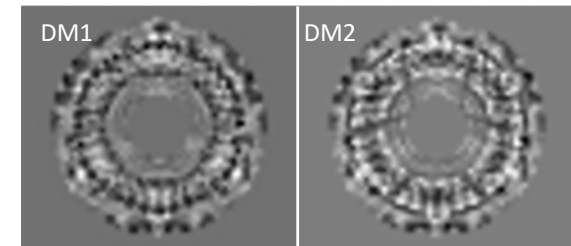


Flight mask designs for the spectroscopy shaped pupil coronagraph.  
Design by A.J. E. Riggs (JPL).

- The baseline CGI design includes four active optics to control the wavefront: a **fast steering mirror (FSM)**, a flat **focusing mirror (FCM)**, and two **deformable mirrors (DM 1 and DM 2)** with 48x48 actuators each.
- High-order wavefront control is implemented by the Electric Field Conjugation (EFC) method. The EFC loop operates on science focal plane data by measuring the interaction of aberrated on-axis starlight with a sequence of DM actuator probes.
- Pointing, focus, and low-order wavefront drifts are sensed by the **Low-Order Wavefront Sensing and Control (LOWFS/C)** subsystem using the Zernike phase-contrast technique on starlight rejected from the occulting mask. Corrections to Zernike modes Z5—Z11 are applied to DM 1.
- The FSM control loop corrects line-of-sight pointing jitter to below 0.95 milliarcsec.



Conceptual diagram of the Zernike phase contrast wavefront sensor (F. Shi, et al., 2016).



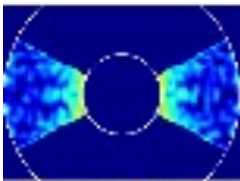
Optimized DM surfaces applied in HLC data simulations.

## References

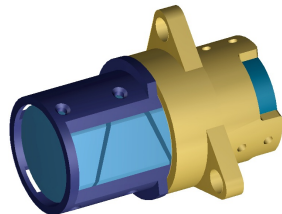
- T. Groff, A. J. E. Riggs, et al., JATIS Vol 2, id 011009 (2015) - <https://doi.org/10.1117/1.JATIS.2.1.011009>
- F. Shi, et al., JATIS Vol 2, id 011021 (2016) - <https://doi.org/10.1117/1.JATIS.2.1.011021>
- J. Krist, et al., JATIS Vol 2, id 011003 (2015) - <https://doi.org/10.1117/1.JATIS.2.1.011003>

# CGI Spectroscopy

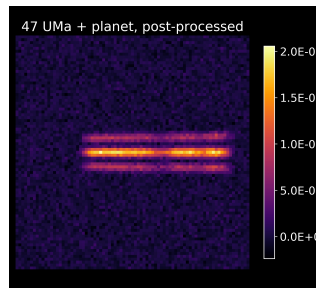
- CGI will be capable of  $R_{\lambda \text{ center}} = 50$  spectroscopy using a slit and Amici prism in Bands 2 and 3



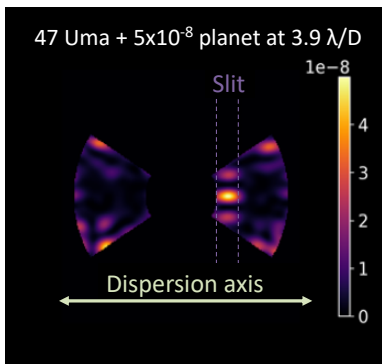
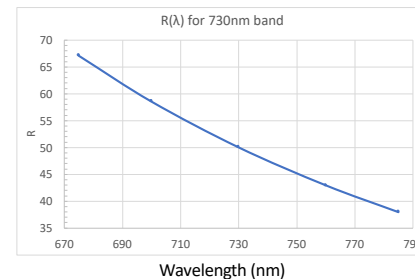
SPC images in 15% band



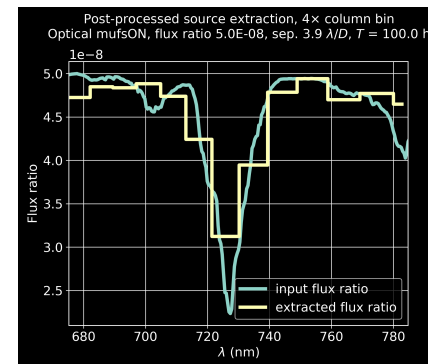
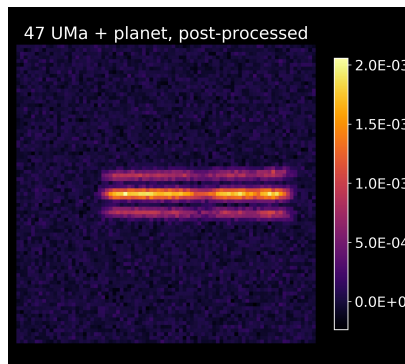
Amici prism



Linear dispersion



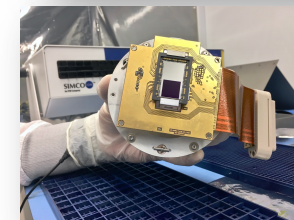
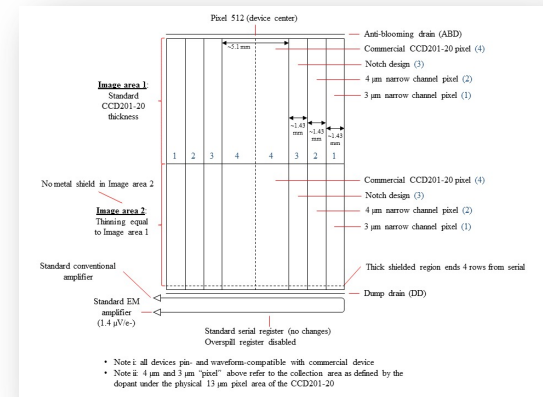
Simulation by Neil Zimmerman



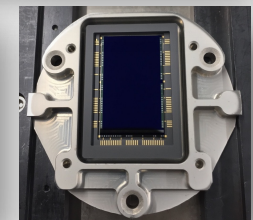
# EMCCD Detectors

- Electron Multiplying CCD (EMCCD) technology is advantageous for a coronagraph application.
  - Programmable gain provides wide dynamic range suitable for bright scenes expected during acquisition and coronagraph configuration, while photon counting capability can be used for faint light observations with zero read noise.
- EMCCD detectors are baselined for direct imaging, spectroscopy and wavefront sensing applications in CGI.
  - Subarray readout suitable for a wavefront sensor application enables 1000 frame- $s^{-1}$  operation to accommodate tip-tilt sensing.
- Work at JPL is focused on low flux characterization with radiation damaged sensors.
  - JPL has invested in modifications to the commercial version of the EMCCD that are expected to improve margins against radiation damage in a flight environment. Prototypes with flight silicon will be delivered in July 2021.
- JPL's EMCCD test lab has measured a low flux threshold of 0.002 c-psf $^{-1}$ -s $^{-1}$ , equivalent to a 32.4 magnitude star through a 2.4m telescope at 500 nm with 10% bandwidth.
  - Devices irradiated to 5 years equivalent life at L2 meet coronagraph technology requirements.

## Radiation-hardened EMCCDs are in Production



Commercial EMCCD



Flight Prototype EMCCD

### References

- [L. Harding, R. Demers, et al., JATIS Vol 2, id 011007 \(2016\)](#)

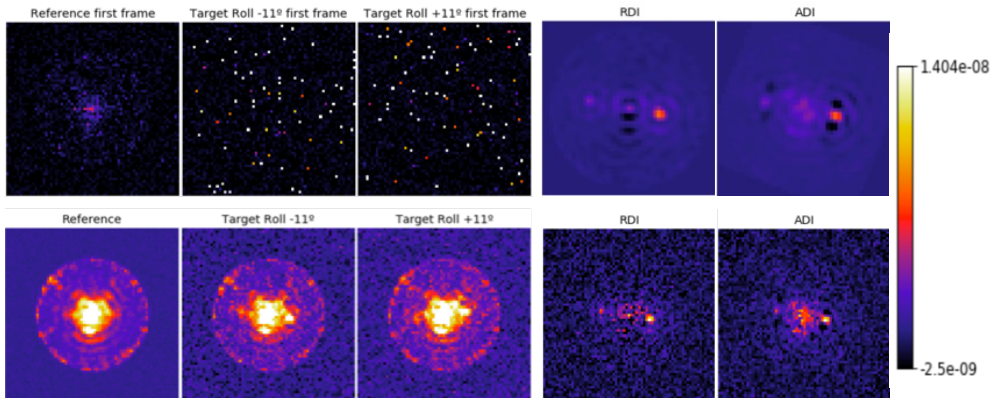


- Investigations on algorithms for CGI data post-processing have encompassed both end-to-end data simulations and analysis of laboratory testbed data.
- Reference differential imaging* (RDI) trials have probed a range of wavefront stability and noise scenarios. Simulations with spacecraft rolls have also enabled tests of *Angular differential imaging* (ADI).

## 1. Post-Processing of OS9 Simulated HLC-Band 1

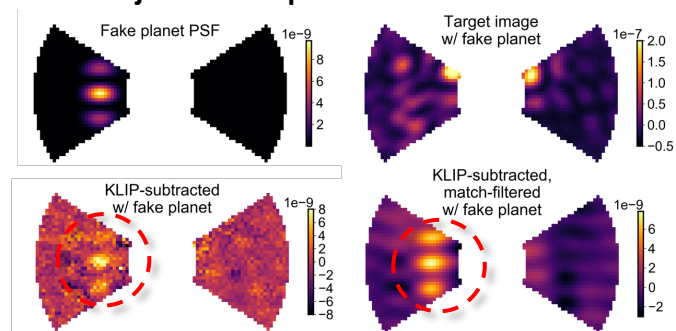
From raw to photon-counted data

Classical PSF subtraction

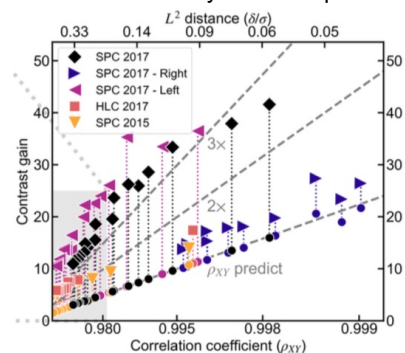


Ygouf et al., 2020

## 2. Laboratory SPC bow-tie frame recorded at HCIT in a static environment (essentially noiseless other than speckles) with injected fake planet at $10^{-8}$ flux ratio



Example application of RDI to SPC data from HCIT, demonstrating the matched-filtered recovery of a fake point source inserted into one image (circled in red)



Left: Post-processing contrast gain plotted against reference library correlation for five datasets. Above a certain correlation coefficient, the post-processing gain is comparable to the gain from classical PSF subtraction.

### References

- M. Ygouf, N. Zimmerman, L. Pueyo, R. Soummer, et al., Proc. SPIE Vol 9904 (2016) - <http://dx.doi.org/10.1117/12.2231581>

# Community Data Challenges

- The WFIRST Exoplanet Data Challenges are a series of blind retrieval exercises based on simulated CGI data to explore instrument capabilities, and inform design choices and operations concepts.
- Imaging challenge launched Oct 20, 2019
  - 6 imaging epochs (4 HLC and 2 SS) of 47 Uma throughout CGI mission
  - At least 1 planet has matching and realistic radial velocity data
  - Extract sources, compute relative photometry & astrometry, disentangle from background sources, exozodiacal light
  - Compute orbital solution using all the information available
  - Teams have 4 months to gradually recover a full exoplanetary system
  - 4 step submission dates: Nov 20, Dec 20, Jan 20, Feb 20
  - [exoplanetdatachallenge.com](http://exoplanetdatachallenge.com)
- 4 tutorial “hackathon events” were organized between March and October 2019 in Baltimore, Pasadena, New York City, and Tokyo

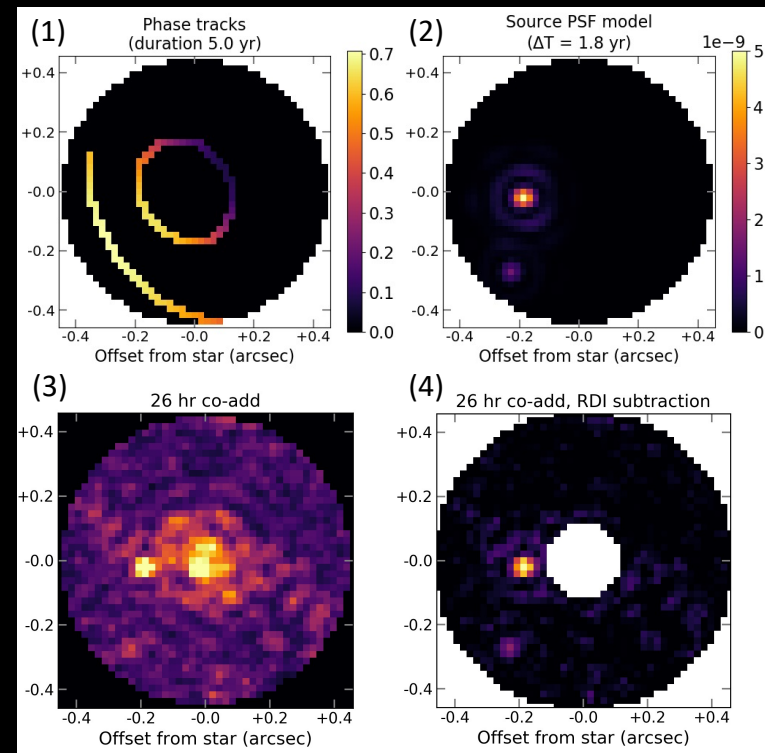
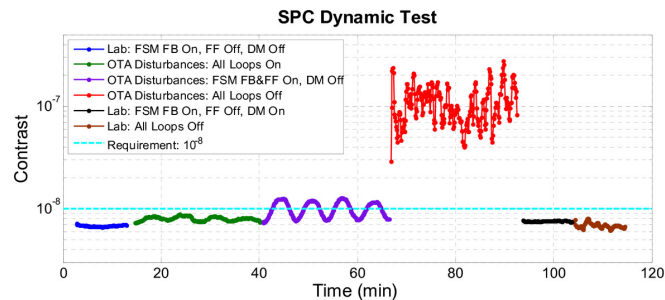


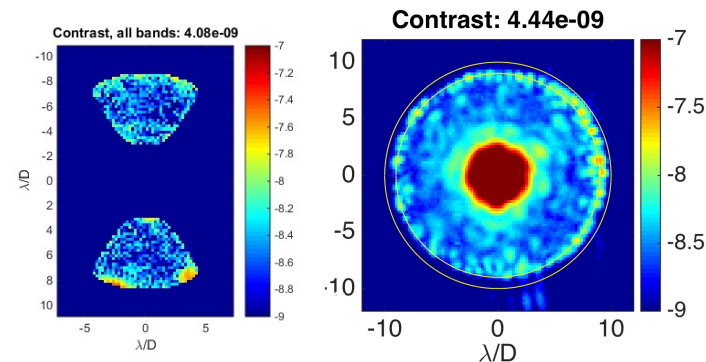
Image data challenge under preparation: (1) Model phase function tracks for a 2-planet system; (2) Source PSF model at one epoch; (3) Simulated co-add based on OS6 HLC time series; (4) Recovery of scene after RDI post-processing.



## Results from the Occulting Mask Coronagraph (OMC) Testbed at JPL HCIT



Dynamic contrast demonstration with a Low Order Wavefront Sensing and Control (LOWFS/C) system integrated on the Occulting Mask Coronagraph testbed. When line-of-sight disturbances and low order wavefront drift (slow varying focus) are introduced on the testbed, the LOWFS senses the pointing error and wavefront drift and corrects them by commanding a fast steering mirror and one of the DMs. Demonstrations with both the SPC and HLC masks surpassed their  $1E-8$  contrast goal (F. Shi, et al., Proc SPIE Vol 10400, 2017).



Normalized intensity maps measured on the OMC testbed in broadband (10 %) light for SPC (left) and HLC. The total contrast between  $3 - 9 \lambda/D$  is listed on top of each figure.

### References

- F. Shi, E. Cady, et al., Proc. SPIE Vol 10400 (2017) - <http://dx.doi.org/10.1117/12.2274887>
- E. Cady, K. Balasubramanian, et al., Proc. SPIE Vol 10400 (2017) - <http://dx.doi.org/10.1117/12.2272834>
- B.-J. Seo, E. Cady, et al., Proc SPIE Vol 10400, 10.1117/12.2274687 (2017) - <http://dx.doi.org/10.1117/12.2274687>
- F. Shi, et al., Proc. SPIE Vol 10698 (2018) - <https://doi.org/10.1117/12.2312746>
- B.-J. Seo, et al, Proc. SPIE Vol 10698 (2018) - <https://doi.org/10.1117/12.2314358>
- D. Marx, et al, Proc. SPIE Vol 10698 (2018) - <https://doi.org/10.1117/12.2312602>
- F. Shi, et al., Proc. SPIE Vol 11117 (2019) - <https://doi.org/10.1117/12.2530486>

# Simulation Resources

Name	Author	Description	Format	URL	References
WFIRST Coronagraph Instrument (CGI) Imaging Simulations	John Krist (JPL)	Time series CGI imaging data simulations produced by JPL, incorporating observatory STOP models and wavefront control.	FITS files	<a href="https://roman.ipac.caltech.edu/sims/Coronagraph_public_images.html">https://roman.ipac.caltech.edu/sims/Coronagraph_public_images.html</a>	J. Krist, et al., JATIS Vol 2, id. 011003 (2016)  J. Krist, et al., Proc SPIE Vol 10400, id. 1040004. (2017)
EXOSIMS	Dmitry Savransky (Cornell U.)	Exoplanet Open-Source Imaging Mission Simulator, with dedicated configurations for simulating CGI surveys and integration times.	web browser interface	<a href="https://roman.ipac.caltech.edu/sims/tools/exosimsCGI/exosimsCGI.html">https://roman.ipac.caltech.edu/sims/tools/exosimsCGI/exosimsCGI.html</a>	D. Savransky & D. Garrett, JATIS Vol 2, id. 011006 (2016)
			Python source code	<a href="https://github.com/dsavransky/EXOSIMS">https://github.com/dsavransky/EXOSIMS</a>	C. Delacroix, D. Savransky, et al., Proc SPIE Vol 9911, id. 991119 (2016)
WebbPSF	Marshall Perrin (STScI)	Simulated Point Spread Functions for WFIRST WFI and CGI (static)	Python source code, with tutorials	<a href="https://github.com/mperrin/webbpsf">https://github.com/mperrin/webbpsf</a>	M. Perrin, et al., Proc SPIE Vol 8442, article id. 84423D (2012) M. Perrin, et al., Proc SPIE Vol 9143, id. 91433X (2014)
CRISPY	Maxime Rizzo (GSFC)	Coronagraph Rapid Imaging Spectrograph in Python - IFS simulations, tools for laboratory testbed demonstrations.	Python source code, with descriptive overview	<a href="https://roman.ipac.caltech.edu/sims/Crispy_simulations.html">https://roman.ipac.caltech.edu/sims/Crispy_simulations.html</a>	M. Rizzo, et al., Proc SPIE Vol 10400, id. 104000B (2017)

# Simulation Resources

Name	Author	Description	Format	URL	References
Fast Linearized Coronagraph Optimizer (FALCO)	AJ Riggs (JPL)	wavefront correction simulator, DM-integrated coronagraph design, testbed operation. CGI simulations	MATLAB and Python3 source codes with Wiki	<a href="https://github.com/ajeldorado/falco-matlab">https://github.com/ajeldorado/falco-matlab</a> <a href="https://github.com/ajeldorado/falco-python">https://github.com/ajeldorado/falco-python</a> <a href="https://github.com/ajeldorado/falco-matlab/wiki">https://github.com/ajeldorado/falco-matlab/wiki</a>	
FALCO + WFIRST CGI PROPER model	AJ Riggs (JPL)	Run end-to-end HOWFSC with the official Phase B model of the WFIRST CGI; Produces: CGI dark hole images and performance tables	MATLAB	<a href="https://github.com/ajeldorado/falco-matlab/wiki/01b%29-Examples-using-the-WFIRST-CGI-PROPER-model">https://github.com/ajeldorado/falco-matlab/wiki/01b%29-Examples-using-the-WFIRST-CGI-PROPER-model</a>	
Starshade Imaging Simulation Toolkit (SISTER)	Sergi R. Hildebrandt (JPL)	produces: end-to-end images of an arbitrary user-defined exoplanetary system and background as observed by a starshade and a telescope	MATLAB	<a href="http://sister.caltech.edu">http://sister.caltech.edu</a>	<a href="#">Hildebrandt et al. 2019, American Astronomical Society Meeting #234, id. 129.01. Bulletin of the American Astronomical Society, Vol. 51, No. 4</a>

Reference	URL	Year
<i>Wide-Field Infrared Survey Telescope-Astrophysics Focused Telescope Assets (WFIRST-AFTA) 2015 Report</i> by the Science Definition Team (SDT) and WFIRST Study Office	<a href="https://roman.gsfc.nasa.gov/science/sdt_public/WFIRST-AFTA_SDT_Report_150310_Final.pdf">https://roman.gsfc.nasa.gov/science/sdt_public/WFIRST-AFTA_SDT_Report_150310_Final.pdf</a>	2015
Journal of Astronomical Telescopes Instruments and Systems, Vol. 2, No. 1, <i>Special Section on WFIRST-AFTA Coronagraphs</i> , eds. Olivier Guyon and Motohide Tamura	<a href="https://www.spiedigitallibrary.org/journals/Journal-of-Astronomical-Telescopes-Instruments-and-Systems/volume-2/issue-01#Editorial">https://www.spiedigitallibrary.org/journals/Journal-of-Astronomical-Telescopes-Instruments-and-Systems/volume-2/issue-01#Editorial</a>	2016
SPIE Proceedings Vol. 10400, <i>Techniques and Instrumentation for Detection of Exoplanets VIII</i> , ed. Stuart Shaklan	<a href="https://www.spiedigitallibrary.org/conference-proceedings-of-spie/10400">https://www.spiedigitallibrary.org/conference-proceedings-of-spie/10400</a>	2017
SPIE Proceedings Vol. 10698, <i>Space Telescopes and Instrumentation 2018: Optical, Infrared, and Millimeter Wave, WFIRST I, II, III</i>	<a href="https://www.spiedigitallibrary.org/conference-proceedings-of-spie/10698">https://www.spiedigitallibrary.org/conference-proceedings-of-spie/10698</a>	2018
<i>Community White Papers submitted to the NAS Exoplanet Science Strategy Committee, co-chairs D. Charbonneau &amp; S. Gaudi. Among the CGI-related papers are: Kasdin et al., Bailey et al., Mennesson et al., Marley et al., B. Crill et al., and others.</i>	<a href="http://sites.nationalacademies.org/SSB/CurrentProjects/SSB_180659">http://sites.nationalacademies.org/SSB/CurrentProjects/SSB_180659</a>	2018
<i>The Wide Field Infrared Survey Telescope: 100 Hubbles for the 2020s</i> , Akeson et al., 2019, <i>Astro2020 white papers</i>	<a href="https://arxiv.org/pdf/1902.05569.pdf">https://arxiv.org/pdf/1902.05569.pdf</a>	2019

- JPL Roman/CGI Website
  - <https://www.jpl.nasa.gov/missions/the-nancy-grace-roman-space-telescope/>
  - CGI Overview and Capability
- Goddard Roman Website
  - <https://roman.gsfc.nasa.gov>
  - Mission Overview
  - Science Overview
  - Resources (images and multimedia, documents, newsroom, and press releases)
- Roman at IPAC
  - <https://roman.ipac.caltech.edu>
  - Science Overview
  - Documentation
  - Simulations (both WFI and CGI)
  - Community Engagement (including Workshops, Meetings and Talks and Preparatory Science)
  - Publications